Temporal solitons in quadratic nonlinear media with opposite group-velocity dispersions at the fundamental and second harmonics

K. Beckwitt,[1,*] Y.-F. Chen,[1] F. W. Wise,[1] and B. A. Malomed[2]
[1]*Department of Applied Physics, Cornell University, 212 Clark Hall, Ithaca, New York 14853, USA*
[2]*Department of Interdisciplinary Studies, Faculty of Engineering, Tel Aviv University, Tel Aviv 69978, Israel*
(Received 14 July 2003; published 20 November 2003)

Temporal solitons in quadratic nonlinear media with *normal* second-harmonic dispersion are studied theoretically. The variational approximation and direct simulations reveal the existence of soliton solutions, and their stability region is identified. Stable solutions are found for large and normal values of the second-harmonic dispersion, and in the presence of large group-velocity mismatch between the fundamental- and second-harmonic fields. The solitons (or solitonlike pulses) are found to have tiny nonlocalized tails in the second-harmonic field, for which an analytic exponential estimate is obtained. The estimate and numerical calculations show that, in the parameter region of experimental relevance, the tails are completely negligible. The results open a way to the experimental observation of quadratic solitons with normal second-harmonic dispersion, and have strong implication to the experimental search for multidimensional ''light bullets.''

DOI: 10.1103/PhysRevE.68.057601 PACS number(s): 42.65.Tg, 42.65.−k

Optical solitons are localized electromagnetic waves that propagate steadily in nonlinear media resulting from a robust balance between nonlinearity and linear broadening due to dispersion and/or diffraction. It is well known that cubic nonlinear materials support temporal solitons [1], but that the resulting balance is unstable to collapse in higher than one dimension [2]. This collapse is arrested in materials with *saturable* nonlinearity [3,4], allowing for the formation of solitons in two and three dimensions (2D and 3D).

Of great interest, theoretically and experimentally, are spatiotemporal solitons (STS) confined in time and both transverse spatial dimensions (''light bullets'') [5]. Unlike temporal solitons, spatial solitons, and quasi-STS (STS confined only in one transverse dimension), light bullets are the only truly stable solitons in a three-dimensional geometry [6]. In addition to their fundamental significance, STS are of interest for their technological applications, as they provide for the possibility of terahertz switching rates when utilized in optical digital logic [7].

In recent years, spatial solitons have been extensively studied in systems with saturable nonlinearity resulting from the photorefractive effect in electro-optic materials [8], and in quadratic nonlinear media, with an effectively saturable nonlinearity resulting from cascaded quadratic processes [9,8]. Theoretically, many kinds of solitons in quadratic nonlinear media have received significant attention (for review see Refs. [10] and [11]). However, quadratic temporal solitons [12] and (2+1)D STS [13,14] have been observed only recently. The main impediment to the formation of temporal solitons (and STS) in quadratic materials is the historically perceived need for large anomalous group-velocity dispersion (GVD) at both the fundamental frequency (FF) and the second harmonic (SH). In particular, the above mentioned experiments utilized anomalous GVD that was induced by angular dispersion from a grating (pulse tilting) to overcome the normal material GVD present at the wavelengths studied. However, pulse-tilting consumes a transverse degree of freedom, preventing soliton confinement along that dimension. This lack of confinement was seen by Liu *et al.* who observed (3+1)D filaments resulting from the transverse instability of (2+1)D STS [15]. These filaments were similar in nature to light bullets, but did not propagate stably due to residual angular dispersion from the pulse tilting technique. To date, all experiments observing temporal solitons and STS in quadratic media have utilized pulse-tilting, so there is significant motivation to generate quadratic temporal solitons in systems without pulse tilt, where the extension to light bullets is possible.

Surveying available quadratic materials leads to the conclusion that large anomalous GVD at the FF is accessible, without significant linear absorption, if this frequency is chosen in the infrared; however, the GVD is accompanied by significant group-velocity mismatch (GVM) between the FF and SH. In addition, in this case the GVD at the SH ranges from near zero to large normal values. So, one is motivated to consider solitons with *normal* GVD at the SH. Recently, STS in the (2+1)D and (3+1)D cases were considered under these conditions [16]. It was found that, for a limited range of parameters, solitons (or solitonlike pulses with tiny nonlocalized tails which would not be experimentally accessible) do exist for normal GVD at the SH and in the presence of some GVM. However, the existence and stability of the more fundamental temporal solitons (i.e., 1D rather than multidimensional pulses) under conditions of normal GVD at the SH has never been considered. This is the subject of the present work.

Temporal solitons in this system are particularly interesting from an experimental standpoint. If observed without the pulse-tilting technique, these would be the crucial step to the formation of true light bullets (either directly through modulation instability in the spatial domain or by launching STS under conditions similar to those for temporal solitons). On the other hand, one would naturally expect the stability re-

*Corresponding author. Electronic address: kb77@cornell.edu

quirements for solitons in 1D to be less stringent than for STS, allowing formation and observation of the solitons over a broader and *more experimentally accessible* range of values of the GVM and normal GVD at the SH.

Below, we present results of both analytical [based on the variational approximation, VA] and direct numerical investigations of temporal solitons in quadratic media with normal GVD at the SH. We show that while the resulting solitary pulses feature the aforementioned nonlocalized tails and thus are not localized in the rigorous sense, with proper choice of the parameters they may be completely localized in any practical sense, so that the resulting waves are indistinguishable from genuine solitons over experimentally accessible propagation lengths. In addition, the pulses are shown to persist in the presence of significant GVM between the FF and SH fields, which is crucial to their experimental observation since *all* quadratic materials give rise to GVM. Solitonlike solutions are demonstrated under accessible experimental parameters, and the implications of the results to the formation of (2+1)D and (3+1)D STS in these systems are discussed.

Within the commonly adopted slowly varying envelope approximation, the coupled equations governing the interaction of the FF and SH field envelopes (u and v, respectively) propagating in the z direction in a medium with quadratic nonlinearity are [6,17]

$$iu_z + u_{\tau\tau} + u^* v - u = 0, \tag{1}$$

$$2i(v_z + \sigma v_\tau) + \delta v_{\tau\tau} + \frac{u^2}{2} - \alpha v = 0. \tag{2}$$

Here u and v are related to the fields E_1 and E_2 (in units of the initial peak FF field E_0) by $E_1 = (u/2)e^{iz}$, $E_2 = v e^{i(\alpha/2)z}$, and $\alpha = 4 - 2\Delta k Z_I$; $\Delta k = k_{2\omega} - 2k_\omega$ is the wave-vector mismatch between the FF and SH fields, and $Z_I = n\lambda/\pi\chi^{(2)}E_0$ characterizes the strength of the nonlinear coupling. The GVM parameter $\sigma = \sqrt{2L_{DS,1}Z_I/L_{GVM}^2}$ is expressed in terms of the dispersion and GVM lengths $L_{DS,j} = \tau_0^2/|\beta_j^{(2)}|$ and $L_{GVM} = c\tau_0/(n_{1,g} - n_{2,g})$, respectively, for material dispersion $\beta_j^{(2)}$ and group-velocity index $n_{j,g}$ at frequency ω_j with $j = 1,2$. Time τ and propagation coordinate z are normalized by $\sqrt{Z_I/2L_{DS,1}}$, and Z_I, respectively. $\delta \equiv 2\beta_2^{(2)}/\beta_1^{(2)}$ is the ratio between the GVD's at the SH and FF. In Eqs. (1) and (2) the GVD at the FF is assumed to be anomalous, so that $\delta > 0$ and $\delta < 0$ correspond, respectively, to anomalous and normal GVD's at the SH. While it is true that soliton solutions are expected with normal GVD at both the FF *and* the SH (and negative nonlinearity), this case is not really different from the usual one. However, the results reported here are equally applicable to the case of normal GVD at the FF and slightly anomalous GVD at the SH, which is also physically realizable in available quadratic media. It is important to note, however, that in the multidimensional case diffraction only has one sign, and the existence of localized solutions demands that the sign of the GVD term in the FF equation [Eq. (1)] be the same as that of diffraction. Hence only the case of anomalous GVD at the FF can give rise to multidimensional solitons.

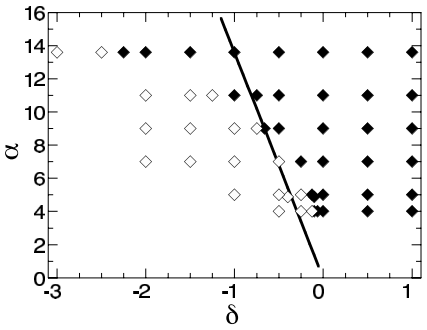

FIG. 1. Stability region for solutions near $\delta = 0$. Filled (empty) diamonds show numerically stable (unstable) solutions. Stability is determined by examining evolution of the solutions over ~ 64 dispersion lengths. The line is the soliton-existence boundary [Eq. (4)], predicted by the VA (stable solutions are predicted to the right of the boundary). Results are for the case of zero GVM ($\sigma = 0$).

Our consideration is broken into three parts: analysis of solutions to Eqs. (1) and (2) using the VA in the zero-GVM limit, numerical simulation of the propagation equations without GVM, and finally a study of the effects of GVM on the resulting solutions.

In the zero-GVM case ($\sigma = 0$), the VA is applied to Eqs. (1) and (2) with $\delta < 0$. Starting with the real Gaussian *ansatz*, $u = A\exp(-\rho\tau^2)$, $v = B\exp(-\gamma\tau^2)$, we arrive at an equation for the temporal-width parameter ρ (cf. Ref. [18]):

$$20\delta\rho^3 + (4\delta - 3\alpha)\rho^2 + 4\alpha\rho - \alpha = 0. \tag{3}$$

Equating the discriminant of Eq. (3) to zero yields the boundary

$$\alpha_0 = \text{const}\cdot\delta, \quad \text{const} \approx -13.6075\ldots, \tag{4}$$

above which (i.e., for $\alpha > \alpha_0$) real solutions exist. Using ρ obtained from Eq. (3) and the underlying Gaussian *ansatz*, we construct an initial guess and employ the shooting method to obtain numerically exact stationary solutions to Eqs. (1) and (2) (see Fig. 3 for a typical example, to be discussed).

The stability of the stationary solutions, which is a critical issue, was tested by direct simulations of Eqs. (1) and (2) using a symmetric split-step beam-propagation method as described in Ref. [14]. Points symbolizing stable and unstable propagation are collected in Fig. 1, along with the soliton-existence boundary, as predicted by the VA in the form of Eq. (4). Gaussian profiles are launched in the numerical simulations (as is further discussed later), and absorptive boundary conditions are employed to suppress energy radiated beyond the calculation window.

The agreement between Eq. (4) and the actual border of the stable solutions, as found from the simulations, is quite reasonable, and is better for small α. With increasing α (which implies approaching the known cascading limit [10,11]), stable solutions are found for somewhat *larger* $|\delta|$ (i.e., larger normal GVD at the SH) than predicted by the VA. Somewhat surprisingly, stable solutions are found for quite large values of $|\delta|$, up to $\delta \sim -2$, with the appropriate choice of α. For instance, Fig. 2 displays stable propagation

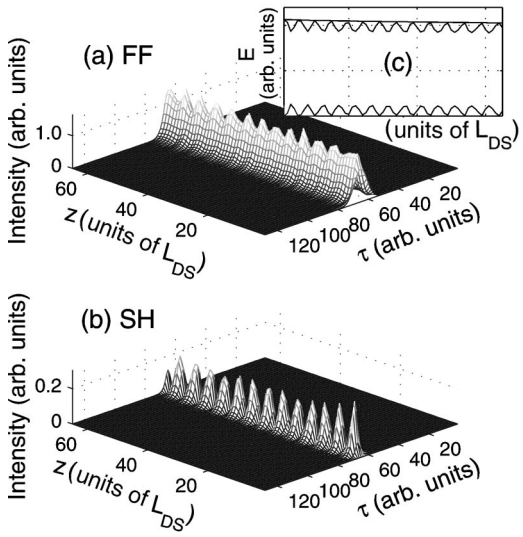

FIG. 2. Evolution of the FF (a) and SH (b) fields for $\alpha=13.6$ and $\delta=-2$. A Gaussian pulse was launched solely in the FF field. Propagation is over ~ 64 dispersion lengths. Inset (c) shows the time-integrated total energy (line), as well as the energy in the FF (upper) and SH (lower) components.

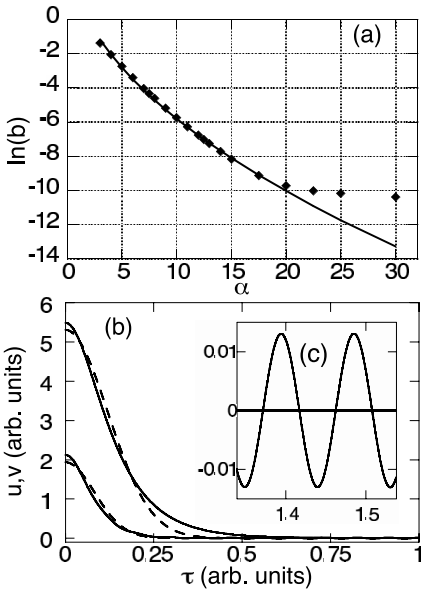

FIG. 3. (a) The amplitude of the cw component (tail) of the SH field (diamonds), as found from the shooting solution of Eq. 3 with $\delta=-0.15$, vs α. The line indicates the predicted dependence in the form of Eq. (5). (b) The shooting results (solid line) and the corresponding VA prediction (dashed line) for u and v (upper and lower traces, respectively) with $\alpha=7.5$. The zoomed region in (c) shows the residual oscillatory SH tail present in (b).

of the solution with $\delta=-2$ [i.e., $\mathrm{GVD}(2\omega)=-\mathrm{GVD}(\omega)$] and $\alpha=13.6$. This is in contrast to the results for the (2+1)D and (3+1)D cases [16], where STS are found to be stable only for much smaller values ($|\delta|\lesssim 0.15$). In Fig. 1, stability is defined by the requirement that less than $\sim 5\%$ of the energy in the formed field is lost after propagation through ~ 64 dispersion lengths; some solutions near the boundary which are characterized as unstable only decay by ~ 5–$20\,\%$ (with the decay increasing further into the normal SH GVD regime).

Despite the robustness of the pulses in numerical simulations, their strict localization must be addressed. This issue is particularly important due to the counter-intuitive nature of stable or even quasistable pulses with normal GVD at the SH. If a small delocalized (continuous wave, cw) component is present in the SH, linearization of Eqs. (1) and (2) shows that it has the form $v=b\cos(\sqrt{(\alpha/|\delta|)}|\tau|+\phi_0)$ where ϕ_0 is an unknown constant, and b is the tail's amplitude. b can be estimated by solving the linearized version of Eq. (1) for u, and using the result to solve Eq. (2) with the source (driving term) $u^2/2$. The source is Fourier transformed, and then its product with the Green's function for the SH field is inverse transformed. Following these lines (cf. Ref. [16], where similar analysis was performed for the multidimensional case), it is possible to isolate a term in the solution representing the cw "tail," and arrive at an estimate for the tail's amplitude,

$$b\sim\exp(-C\sqrt{\alpha/|\delta|}), \tag{5}$$

where C is an unknown constant.

To test Eq. (5) we use the shooting method as described above with $\delta=-0.15$ and various values of α [numerical error of the shooting method is estimated to be $\sim O(10^{-5})$]. Figure 3 shows the dependence of the resulting tail's amplitude on α, along with a fit to Eq. (5). Up to $\alpha\approx 20$, the decay of the tail amplitude follows Eq. (5) closely. For still larger α, the tail amplitude b decays slower.

The presence of the tail means that the solutions found are not strictly localized; however, for appropriate α and δ the SH peak-to-tail ratio can be easily made $\gtrsim 10^4$. This explains why no decay is observed in Fig. 2 (and in simulations of other stable solutions with $\delta<0$ in Fig. 1). Pulses with an exponentially small cw component will appear as true solitons in any feasible experiment. The conditions under which the tails are minimized (large α) correspond precisely to the transition to an effective Kerr-like medium in the cascading limit, when the sign of the SH dispersion is not significant. Notice also the close proximity of the numerical solutions to the Gaussian *ansatz*. Based on this, Gaussian profiles are launched in numerical simulations.

It is also necessary to address the effect of GVM (σ) on the stability of the solutions. Numerically, we study the effects of GVM by direct simulations, starting from a point in the (α,δ) plane with known stable solution for $\sigma=0$, and increasing σ. Figure 4 shows the stable solution at $\alpha=13.6$, $\delta=-0.5$, with increasing GVM. It is apparent from the figure that small GVM ($\sigma\lesssim 2$) has little effect on the stability of the solution. Remarkably, some of the soliton keeps a part of its energy for GVM up to $\sigma\sim 30$. This is unlike in higher dimensions [16], where GVM very quickly destabilizes the solitons. At conditions that correspond to realistic experimental parameters in quadratic nonlinear media, this corresponds to GVM of several picosecond/millimeter.

This result greatly increases the chance of observing the solitons experimentally. Values of the normalized parameters

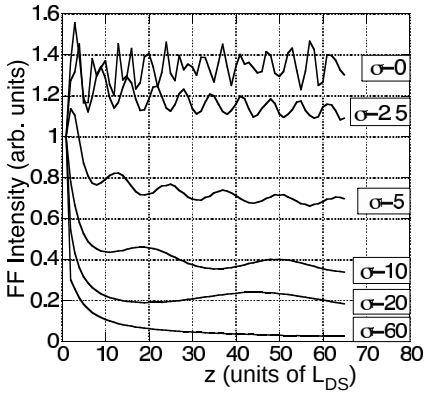

FIG. 4. Peak FF profiles showing effects of increased GVM on soliton formation at $\alpha=13.6$ and $\delta=-0.5$. Up to $\sigma\approx1.2$ profile shows no decay. As in Figs. 1 and 2, a Gaussian FF profile is launched.

for the commonly used quadratic material periodically poled lithium niobate in the infrared (at $\lambda\sim3$ μm) are $\alpha\approx12$, $\delta\approx-0.5$, and $\sigma\approx1.3$, which are well within the effective stability range found above for the solitons. The initial point in (α, δ) used in Fig. 4 was picked from the stability region of Fig. 1. Starting closer to the boundary yields somewhat less resilience to GVM, as expected.

While realistic material parameters most likely necessitate working with $\sigma>0$, solitonlike solutions with normal GVD at the SH present a new degree of freedom in the space of experimental parameters. In particular, most available quadratic media have a zero GVM point in the infrared, but at wavelengths corresponding to large normal GVD at the SH. Thus, the ability to work with normal SH dispersion could allow experimental study of solitons with *zero* GVM (in addition to large values of σ). Given present materials this is unlikely to apply to STS, where the requirements on δ are much more restrictive.

In summary we have demonstrated that quadratic nonlinear media support temporal solitons with normal GVD at the SH. Formally, these solutions are not strictly localized, however, with appropriate choice of the parameters, the residual cw tail in the SH field can be reduced to $\lesssim10^{-4}$ of the soliton's amplitude. Experimentally there should be no detectable difference between these and true soliton solutions over measurable propagation lengths. Numerically, the soliton solutions survive even in the presence of significant GVM. This should provide an important medium for the study of quadratic solitons in the temporal and, eventually, spatiotemporal domains.

This work was supported by the National Science Foundation under Grant No. PHY-0099564, and the Binational (U.S.-Israel) Science Foundation (Contract No. 1999459). We thank D. Mihalache, A. V. Buryak, L. Torner, I. N. Towers, L. Qian, and H. Zhu for valuable discussions. Computational facilities were provided by the Cornell Center for Materials Research and the Cornell Theory Center.

[1] G.P. Agrawal, *Nonlinear Fiber Optics* (Academic Press, San Diego, 1995).
[2] V.E. Zakharov and A.M. Rubenchik, Zh. Éksp. Teor. Fiz. **65**, 997 (1973) [Sov. Phys. JETP **38**, 494 (1974)].
[3] A.B. Blagoeva, S.G. Dinev, A.A. Dreischuh, and A. Naidenov, IEEE J. Quantum Electron. **QE-27**, 2060 (1991).
[4] D.E. Edmundson and R.H. Enns, Opt. Lett. **17**, 586 (1992).
[5] Y. Silberberg, Opt. Lett. **15**, 1282 (1990).
[6] A.A. Kanashov and A.M. Rubenchik, Physica D **4**, 122 (1981).
[7] R. McLeod, K. Wagner, and S. Blair, Phys. Rev. A **52**, 3254 (1995).
[8] G.I. Stegeman and M. Segev, Science **286**, 1518 (1999).
[9] R. DeSalvo, D.J. Hagan, M. Sheik-Bahae, G. Stegeman, E.W. Van Stryland, and H. Vanherzeele, Opt. Lett. **17**, 28 (1992).
[10] C. Etrich, F. Lederer, B.A. Malomed, T. Peschel, and U. Peschel, Prog. Opt. **41**, 483 (2000).
[11] A.V. Buryak, P. Di Trapani, D.V. Skryabin, and S. Trillo, Phys. Rep. **370**, 63 (2002).
[12] G. Valiulis, A. Dubietis, R. Danielius, D. Caironi, A. Visconti, and P. Di Trapani, J. Opt. Soc. Am. B **16**, 722 (1999).
[13] X. Liu, L.J. Qian, and F.W. Wise, Phys. Rev. Lett. **82**, 4631 (1999).
[14] X. Liu, K. Beckwitt, and F.W. Wise, Phys. Rev. E **62**, 1328 (2000).
[15] X. Liu, K. Beckwitt, and F.W. Wise, Phys. Rev. Lett. **85**, 1871 (2000).
[16] I.N. Towers, B.A. Malomed, and F.W. Wise, Phys. Rev. Lett. **90**, 123902 (2003).
[17] B.A. Malomed, P. Drummond, H. He, A. Berntson, D. Anderson, and M. Lisak, Phys. Rev. E **56**, 4725 (1997).
[18] V. Steblina, Yu.S. Kivshar, M. Lisak, and B.A. Malomed, Opt. Commun. **118**, 345 (1995).